Turkish Journal of Electrical Engineering & Computer Sciences

http://journals.tubitak.gov.tr/elektrik/

Research Article

Turk J Elec Eng & Comp Sci
(2013) 21: 980 – 1001

doi:10.3906/elk-1112-49

On-line self-learning PID controller design of SSSC using self-recurrent wavelet neural networks

Soheil GANJEFAR,* **Mojtaba ALIZADEH**
Department of Electrical Engineering, Bu-Ali Sina University, Hamedan, Iran

Received: 13.12.2011 • **Accepted:** 29.01.2012 • **Published Online:** 03.06.2013 • **Printed:** 24.06.2013

Abstract: Conventionally, FACTS devices employ a proportional-integral (PI) controller as a supplementary controller. However, the conventional PI controller has many disadvantages. The present paper aims to propose an on-line self-learning PI-derivative (PID) controller design of a static synchronous series compensator for power system stability enhancement and to overcome the PI controller problems. Unlike the PI controllers, the proposed PID controller has a local nature because of its powerful adaption process, which is based on the back-propagation (BP) algorithm that is carried out through an adaptive self-recurrent wavelet neural network identifier (ASRWNNI). In fact, the PID controller parameters are updated in on-line mode using the BP algorithm based on the information provided by the ASRWNNI, which is a powerful and fast-acting identifier thanks to its local nature, self-recurrent structure, and stable training algorithm with adaptive learning rates based on the discrete Lyapunov stability theorem. The proposed control scheme is applied to a 2-machine, 2-area power system under different operating conditions and disturbances to demonstrate its effectiveness and robustness. Later on, the design problem is extended to a 4-machine, 2-area benchmark system and the results show that the interarea modes of the oscillations are well damped with the proposed approach.

Key words: Adaptive control, flexible AC transmission systems, power system control, power system stability, self-recurrent wavelet neural networks

1. Introduction

Power systems can be studied as highly nonlinear large-scale dynamic systems [1]. Electromechanical oscillations occur when the power system is subjected to disturbances. Power system stabilizers (PSSs) are conventionally employed for power system oscillation damping. However, they have many disadvantages; they can be adversely affected by the voltage profile while the system is operating at a leading power factor. Moreover, during a severe disturbance, their suppressing ability may be degraded [2,3].

The recent development of power electronics has attracted more attention to the use of flexible AC transmission system (FACTS) devices in power systems with the aim of damping the oscillations and improving the dynamic stability of the power system [4–11]. The suitably controlled FACTS devices can provide good damping to both the interarea and the local mode oscillations of a multimachine power system.

Conventionally, FACTS devices employ a proportional-integral (PI) controller as a supplementary controller [12]. The PI controller is used in a wide range of industrial applications due to its simple structure and low cost. However, the PI-type controller has many disadvantages, which are more highlighted when the controlled object is highly nonlinear. In this situation, the PI controller is almost a deficient controller, and

*Correspondence: s_ganjefar@basu.ac.ir

its deficiency is mainly related to its tuning method as the first problem and its static nature as the second problem.

To overcome the first problem, many different parameter tuning methods have been presented for PI/PI-derivative (PID) controllers. A survey conducted up until 2002 was given in [13,14]. These methods are generally modifications of the frequency response method proposed by Ziegler and Nichols [15]. Numerous analytical-based works were also presented in order to tune the PI/PID parameters [16–18]. Robust and optimal control methods were also proposed to design the PI/PID controllers [19–23]. Recently, as other alternatives to PID tuning, modern heuristic optimization techniques such as simulated annealing [24], the evolutionary algorithm [25], particle swarm optimization [26], and chaotic optimization [27] have been given much attention. Most of these works propose a fixed-gain PI/PID controller with an unappealing static nature (the second problem).

The present paper aims to propose an on-line self-learning PID (OLSL-PID) controller for a static synchronous series compensator (SSSC) for power system stability enhancement and to overcome the PI controller problems. Unlike the PI controllers, the proposed PID controller has a local behavior because of its powerful adaption process, which is based on the back-propagation (BP) algorithm. During the adaption process, the Jacobian of the plant is also needed. Generally, 2 control strategies can be used to evaluate the Jacobian, 'direct adaptive control' and 'indirect adaptive control'. In this paper, it is calculated based on the indirect adaptive control theory. An on-line identification algorithm is therefore required to evaluate the Jacobian on-line.

Multilayer perceptron (MLP) networks, based on the gradient descent (GD) training algorithm with static learning rates, are used by many researchers for the identification of synchronous generators [28–32]. However, MLPs have some drawbacks due to their inherent characteristics [33]. They have a global nature due to their use of the continued activation function. This global nature slows the speed of learning and results in the essence of the local minimum. Recently, wavelet neural networks (WNNs), which absorb the advantages such as the multiresolution of the wavelets and the learning of the MLP, were used to identify the nonlinear systems [34–38]. The WNN is suitable for the approximation of unknown nonlinear functions with local nonlinearities and fast variations because of its intrinsic properties of finite support and self-similarity [39]. Aside from these advantages, the WNN has a shortcoming; due to its feed-forward network structure, it can only be used for static problems. Hence, self-recurrent wavelet neural networks (SRWNNs), which combine such features as the dynamics of the recurrent neural network and the fast convergence of the WNN, were proposed to identify the nonlinear systems [33–40].

In this article a SRWNN is thus used as an identifier to adapt the PID controller parameters. Moreover, the GD method using adaptive learning rates (ALRs) is applied to train all of the weights of the adaptive SRWNN identifier (ASRWNNI). The proposed control scheme is applied to a 2-machine, 2-area power system under different operating conditions and disturbances to demonstrate its effectiveness and robustness. Nonlinear simulation results are also presented to highlight the promising features of the proposed controller. Later on, the design problem is extended to a 4-machine, 2-area system and the results show that the interarea modes of the oscillations are well damped with the proposed approach.

The reminder of the paper is organized as follows: the 2-machine, 2-area power system model is presented in Section 2. The design of the OLSL-PID controller is described in Section 3. The SRWNN structure and its application to the adaptive identifier design are presented in Section 4. The convergence analysis for the ASRWNNI is provided in Section 5. The simulation results are discussed in Section 6. Section 7 gives the conclusion with a brief summary of the simulation results.

2. The 2-machine, 2-area power system with SSSC

To assess the effectiveness and robustness of the proposed approach, a 2-machine, 2-area power system equipped with a SSSC, shown in Figure 1, is considered. It consists of 2 generators and 1 major load center of approximately 2200 MW at bus 3, which is modeled using a dynamic load model where the active and reactive power absorbed by the load is a function of the system voltage. Each generator is equipped with a PSS. A 100-MVA SSSC is also installed at bus 1, in series with line L_1. The system data are given in Appendix A.

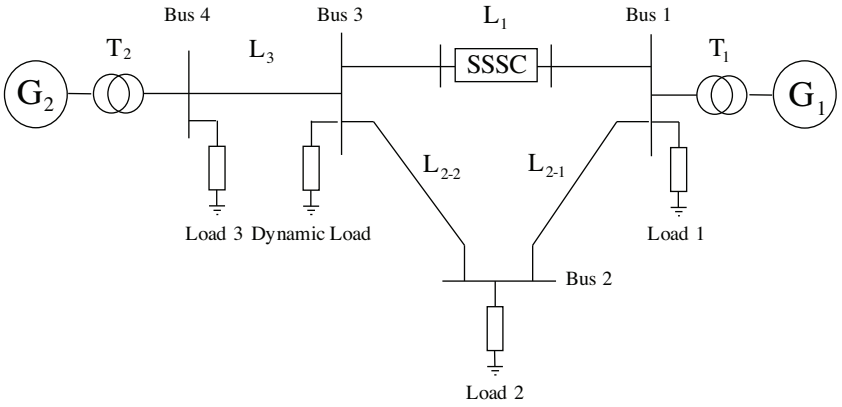

Figure 1. The 2-machine power system with SSSC.

3. OLSL-PID controller design

In this paper, an adaption law based on the BP algorithm is used to tune the PID gains in on-line mode. The general structure of the control system is shown in Figure 2. The PID output is the control action $u(n)$. To tune the PID controller gains, it can be considered as a single layer perceptron (SLP) neural network with the linear activation function 'purelin'. Figure 3 represents the PID controller based on the neural network. Hence, the PID controller gains can also be considered as the weights of the SLP neural network.

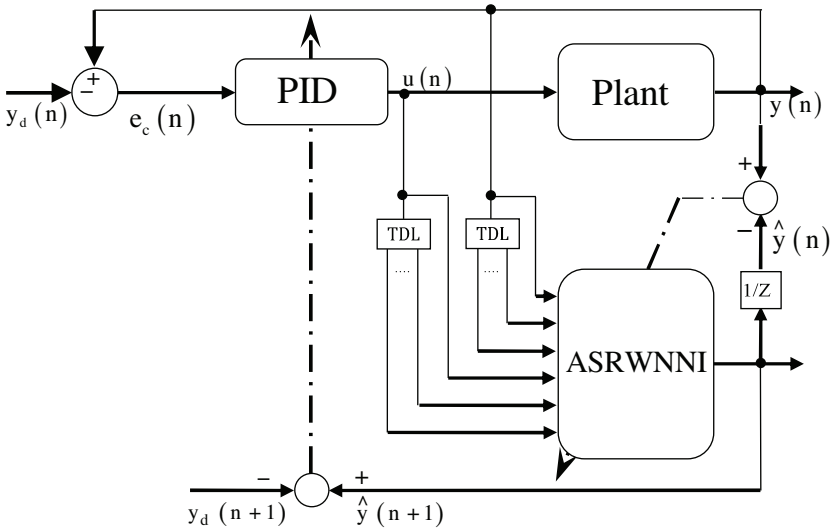

Figure 2. Control system structure.

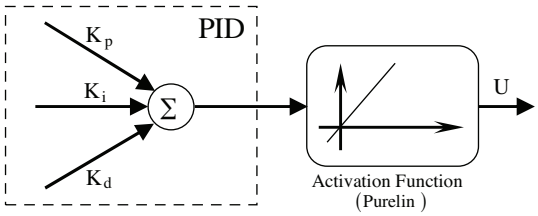

Figure 3. The PID controller based on the neural network.

These gains can therefore be updated on-line using the BP algorithm. To select the optimal control signal, the following cost function can be considered:

$$J_c(n) = \frac{1}{2}\left[y(n) - y_d(n)\right]^2 = \frac{1}{2}e_c^2(n), \tag{1}$$

where $y(n)$ is the plant output and $y_d(n)$ is the desired plant output, both at time step n. To minimize the cost function in Eq. (1), the PID controller gains are adjusted on-line using the GD method. The GD method may be defined as:

$$W_c^i(n+1) = W_c^i(n) + \eta_c^i\left(-\frac{\partial J_c(n)}{\partial W_c^i(n)}\right), \tag{2}$$

where for $W_c = [K_p, K_i, K_d]$ and $\eta_c = [\eta^{Kp}, \eta^{Ki}, \eta^{Kd}]$, W_c^i and η_c^i, respectively, represent an arbitrary gain and the corresponding learning rate in the PID controller. The partial derivative of the cost function in Eq. (1) with respect to W_c^i is:

$$\frac{\partial J_c(n)}{\partial W_c^i(n)} = \left[e_c(n)\frac{\partial y(n)}{\partial u(n)}\right]\frac{\partial u(n)}{\partial W_c^i(n)}. \tag{3}$$

The components of the weighting vector are also as follows:

$$\frac{\partial u(n)}{\partial K_p} = e_c, \tag{4}$$

$$\frac{\partial u(n)}{\partial K_i} = \int_0^{t_{current}} e_c.dt, \tag{5}$$

$$\frac{\partial u(n)}{\partial K_d} = \frac{d}{dt}e_c, \tag{6}$$

where $\partial y(n)/\partial u(n)$ in Eq. (3) is the plant Jacobian in each time step n. Regarding what has been mentioned so far, the ASRWNNI is used to evaluate the Jacobian on-line. Adjustment of the cycle of the OLSL-PID for each time step n is given in Appendix B.

4. The ASRWNNI

As mentioned before, the Jacobian of the plant is needed during the adaption process. In this section, the SRWNN is adapted to design an adaptive plant identifier. This identifier can then be used to evaluate the Jacobian on-line, based on the indirect adaptive control theory.

4.1. The SRWNN structure

The detailed structure of the SRWNN, consisting of 4 layers with N_i inputs, 1 output, and $N_i \times N_w$ mother wavelets, is shown in Figure 4 [40]. Layer 1 is an input layer. Layer 2 is a mother wavelet layer. Each node of this layer has a mother wavelet, with the first derivative of a Gaussian function $\varphi(x) = x\times\ \exp(-0.5\ \times x^2)$ as a mother wavelet function, and a self-feedback loop. Each wavelet (wavelon) φ_{ij} is derived from its mother wavelet φ as follows:

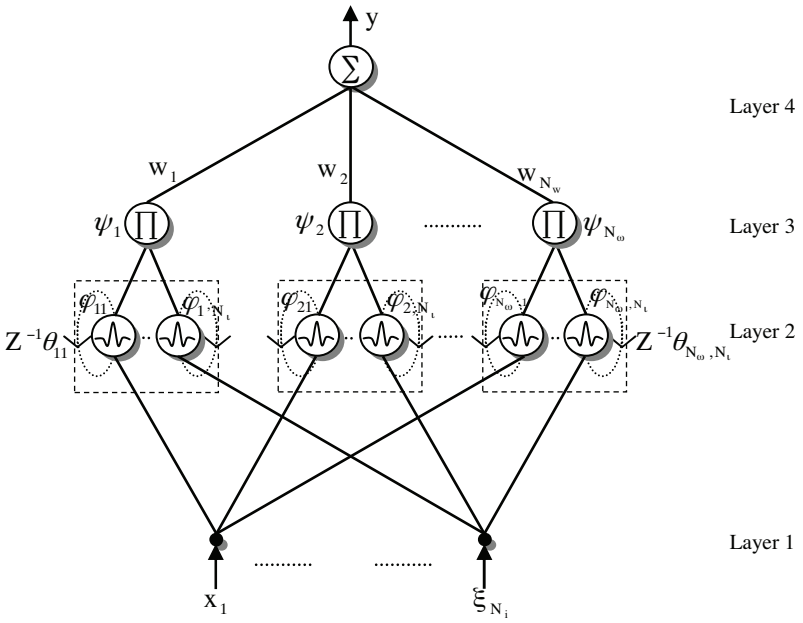

Figure 4. The SRWNN structure.

$$\phi_{ij}\left(z_{ij}\right) = \phi\left(z_{ij}\right), \forall z_{ij} = \left(\left(u_{ij} - t_{ij}\right)/d_{ij}\right), \tag{7}$$

where t_{ij} and d_{ij} are the wavelet translation factor and the dilation factor, respectively. The subscript ij indicates the jth input term of the ith wavelet. Moreover:

$$u_{ij}\left(n\right) = x_j\left(n\right) + \phi_{ij}\left(n-1\right)\theta_{ij},$$

where θ_{ij} shows the weight of the self-feedback loop. Layer 3 is a product layer. The nodes in this layer are given as follows:

$$\psi_i = \prod_{j=1}^{N_i} \phi\left(z_{ij}\right) = \prod_{j=1}^{N_i} \left[\left(z_{ij}\right) exp\left(-\frac{1}{2} z_{ij}^2\right)\right]. \tag{8}$$

The network output is finally calculated as:

$$y\left(n\right) = \sum_{i=1}^{N_w} w_i \psi_i, \tag{9}$$

where w_i is the connection weight between the product nodes and the output nodes.

4.2. Application of the SRWNN for the plant identification

The ASRWNNI, based on the series-parallel method [41], can be represented as:

$$x_I = [y(n), y(n-1), ..., y(n-p), u(n), u(n-1), ..., u(n-q)], \tag{10}$$

$$\hat{y}(n+1) = f_I(x_I), \tag{11}$$

where $\hat{y}(n+1)$ is the predicted speed deviation at time step $n+1$ and x_I is the input of the ASRWNNI. Moreover, p and q indicate the number of past output and past input state variables, respectively. Here, both p and q are chosen to be 1. Our goal is to minimize the following quadratic cost function in both on-line and off-line modes:

$$J_I(n) = \frac{1}{2}(y(n) - \hat{y}(n))^2 = \frac{1}{2}e_I(n)^2. \tag{12}$$

Using the GD method, the weight values of the SRWNN are adjusted as follows:

$$W_I^i(n+1) = W_I^i(n) + \eta^i \left(-\frac{\partial J_I(n)}{\partial W_I^i(n)}\right), \tag{13}$$

where for $W_I = [t_{ij}, d_{ij}, \theta_{ij}, w_i]$ and $\eta_I = [\eta^t, \eta^d, \eta^\theta, \eta^w]$, W_I and η_I^i, respectively, represent an arbitrary weight and the corresponding learning rate in the SRWNNI. The partial derivative of the cost function with respect to W_I^i is:

$$\frac{\partial J_I(n)}{\partial W_I^i(n)} = e_I(n)\frac{\partial e_I(n)}{\partial W_I^i(n)} = -e_I(n)\frac{\partial \hat{y}(n)}{\partial W_I^i(n)}.$$

The components of the weighting vector are as follows:

$$\frac{\partial \hat{y}(n)}{\partial t_{ij}(n)} = w_i\psi_i\left(\frac{-1}{d_{ij}}\right)\left(\frac{1}{z_{ij}} - z_{ij}\right), \tag{14}$$

$$\frac{\partial \hat{y}(n)}{\partial d_{ij}(n)} = z_{ij}\left(\frac{\partial \hat{y}(n)}{\partial t_{ij}(n)}\right), \tag{15}$$

$$\frac{\partial \hat{y}(n)}{\partial \theta_{ij}(n)} = -(\phi_{ij}(n-1))\left(\frac{\partial \hat{y}(n)}{\partial t_{ij}(n)}\right), \tag{16}$$

$$\frac{\partial \hat{y}(n)}{\partial w_i(n)} = \psi_i. \tag{17}$$

Hence, this identifier can be used for calculating the system sensitivity in each time step n as:

$$\frac{\partial y(n+1)}{\partial u(n)} \approx \frac{\partial \hat{y}(n+1)}{\partial x_I}\frac{\partial x_I}{\partial u(n)}. \tag{18}$$

From Eq. (10), $\partial x_I / \partial u(n)$ can be written as [42]:

$$\frac{\partial x_I}{\partial u(n)} = [0\ 0\ , ...,\ 1\ f_1(z)\ , ..., f_q(z)]^T, \tag{19}$$

where $f_i(z) = z^{-i}$, and

$$\frac{\partial \hat{y}(n+1)}{\partial x_{I,j}} = \sum_{i=1}^{N_w} w_{i\times}\psi_i\left(\frac{1}{d_{ij}}\right)\left(\frac{1}{z_{ij}} - z_{ij}\right). \tag{20}$$

5. Convergence analysis for the ASRWNNI

It is important to find the optimal learning rate in an on-line mode because despite the fact that the convergence is guaranteed for the small values of the learning rate, it should be noted that the speed is very slow. Moreover, the algorithm becomes unstable for the big values of the learning rate; thus, in this section, the convergence analysis of the proposed identifier is presented by several theorems.

Theorem 1. Let η_I^i be the learning rate for the weights of the ASRWNNI; let g_{max}^i be defined as $g_{max}^i = \max_n ||g^i(n)||$, where $g^i(n) = \partial\hat{y}(n) / \partial W_I^i$ and $||.||$ is the usual Euclidean norm in $\Re^n$; then the convergence is guaranteed if η_I^i is chosen as:

$$0 < \eta_I^i < 2/\left(g_{\max}^i\right)^2. \tag{21}$$

Proof. See Appendix C.

Theorem 2. Let η_I^w be the learning rate for the weight w_I of the ASRWNNI. Next, the convergence is guaranteed if the learning rate satisfies $0 < \eta_I^w < 2/N_w$.

Proof: See Appendix D.

Theorem 3. Let η_I^t, η_I^d, and η_I^θ be the learning rates of the translation, dilation, and self-feedback weights for the ASRWNNI in the indirect adaptive control structure, respectively. The convergence is guaranteed if the learning rates satisfy:

$$0 < \eta_I^t < \frac{2}{N_w N_i}\left[\frac{|d|_{\min}}{|w|_{\max} \times 2\exp(-0.5)}\right]^2, \tag{22}$$

$$0 < \eta_I^d < \frac{2}{N_w N_i}\left[\frac{|d|_{\min}}{|w|_{\max} \times 2\exp(0.5)}\right]^2, \tag{23}$$

$$0 < \eta_I^\theta < \frac{2}{N_w N_i}\left[\frac{|d|_{\min}}{|w|_{\max} \times 2\exp(-0.5)}\right]^2. \tag{24}$$

Proof: See Appendix E.

Remark 1. The maximum learning rate that guarantees the most rapid or optimal convergence corresponds to [33]:

$$\eta_I^{w,\max} = \frac{1}{N_w}, \tag{25}$$

$$\eta_I^{t,\max} = \eta_I^{\theta,\max} = \frac{1}{N_w N_i}\left[\frac{|d|_{\min}}{|w|_{\max} \times 2\exp(-0.5)}\right]^2, \tag{26}$$

$$\eta_I^{d,\max} = \frac{1}{N_w N_i}\left[\frac{|d|_{\min}}{|w|_{\max} \times 2\exp(0.5)}\right]^2. \tag{27}$$

It should be noted that in all of the studies in this section, the assumption was that the network's data are not normalized. Obviously, the obtained equations should be generalized for when the data have been normalized.

6. Simulation results and discussion

6.1. Preliminary

In this section, simulation studies are conducted for the example power system subjected to both severe and small disturbances under different operating conditions. The results are presented in 3 cases and 2 operating points, as shown in the Table.

Table. Operating conditions.

Cases	P_1	Q_1	P_2	Q_2	$P_{dynamicload}$	$Q_{dynamicload}$
OP_1	0.7619	–0.0478	0.7509	0.0513	1.5711	0.0718
OP_2	0.8589	0.0539	1	0.0750	1.9981	0.1076

These cases are also as follows: first without a controller (NC), second with the fixed-gain PI controller, and third with the OLSL-PID controller. The PI controller is initially tuned, carefully. Afterwards, its parameters are kept unchanged for all of the performed tests. The PI gains are given in Appendix F.

The single-line block diagram of the SSSC control system with an OLSL-PID controller is shown in Figure 5.

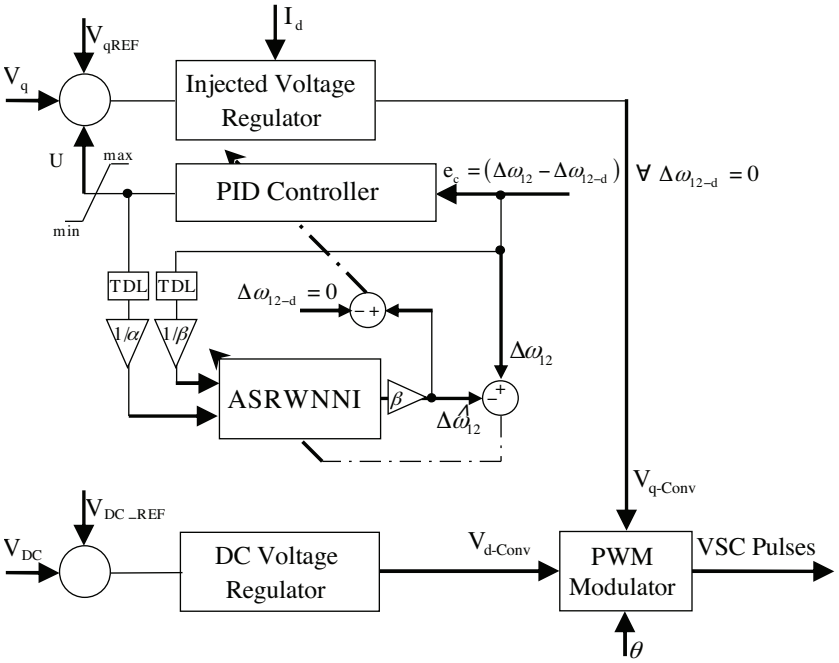

Figure 5. Single-line diagram of the SSSC control system with an OLSL-PID controller.

Our simulation studies show that a 2-order identifier is accurate enough to calculate the Jacobian of the example power system on-line, meaning that the ASRWNNI has 4, 32, 8, and 1 neurons at the input, mother wavelet, wavelet, and output layers, respectively. It should be noted that the input and output signals of the ASRWNNI are scaled to the range of [–1, 1] using parameters α and β (here $\alpha = 0.15$ and $\beta = 0.007$).

First, the ASRWNNI is trained off-line over a wide range of operating conditions and disturbances. During this phase, the input and the desired output of the ASRWNNI are $[\Delta\omega(n-1),\ \Delta\omega(n-2),\ u(n\text{-}1),\ u(n\text{-}2)]$ and $\Delta\omega(n)$, respectively. Later on, the ASRWNNI is placed in the system, as shown in Figures 2 and 5. During this phase, the input and desired output of the ASRWNNI are $[\Delta\omega(n),\ \Delta\omega(n-1),\ u(n),\ u(n-1)]$ and

$\Delta\omega(n+1)$, respectively. Furthermore, the on-line training of the ASRWNNI is performed in every sampling period using the BP algorithm with ALRs.

The difference in the speed deviations of the generators in the 2 areas $(\omega_1 - \omega_2)$ is chosen as the control input of the PID in this paper. All of the PID gains are initially set to those of the conventional PI controller. Eventually, the PID controller is placed in the system and its parameters are updated in on-line mode using the BP algorithm, based on the information provided by the ASRWNNI.

For the adaptive controller implementation, a sampling rate is also needed. Such factors as the ability of controller, the ability of controller's adaption law, the complexity of the plant, and so on have effects on the selection of the sampling rate. Hence, the sampling rate selection problem does not follow any systematic approaches; it is based on trial and error. In this paper, based on our trial-and-error studies, a sampling rate of 40 Hz is selected.

6.2. Nonlinear time-domain simulation

6.2.1. The results at OP_1

To assess the effectiveness of the proposed controller under transient conditions, the 3-phase fault of a 10-cycle duration at bus 1 is selected as the first disturbance. The results include the system responses and identifier performance, as presented in Figure 6. It is evident from the results that the OLSL-PID provides better damping performance than the PI controller, significantly improving the transient stability performance of the example power system thanks to intelligent variations of its gains, while the ASRWNNI provides a promising tracking performance.

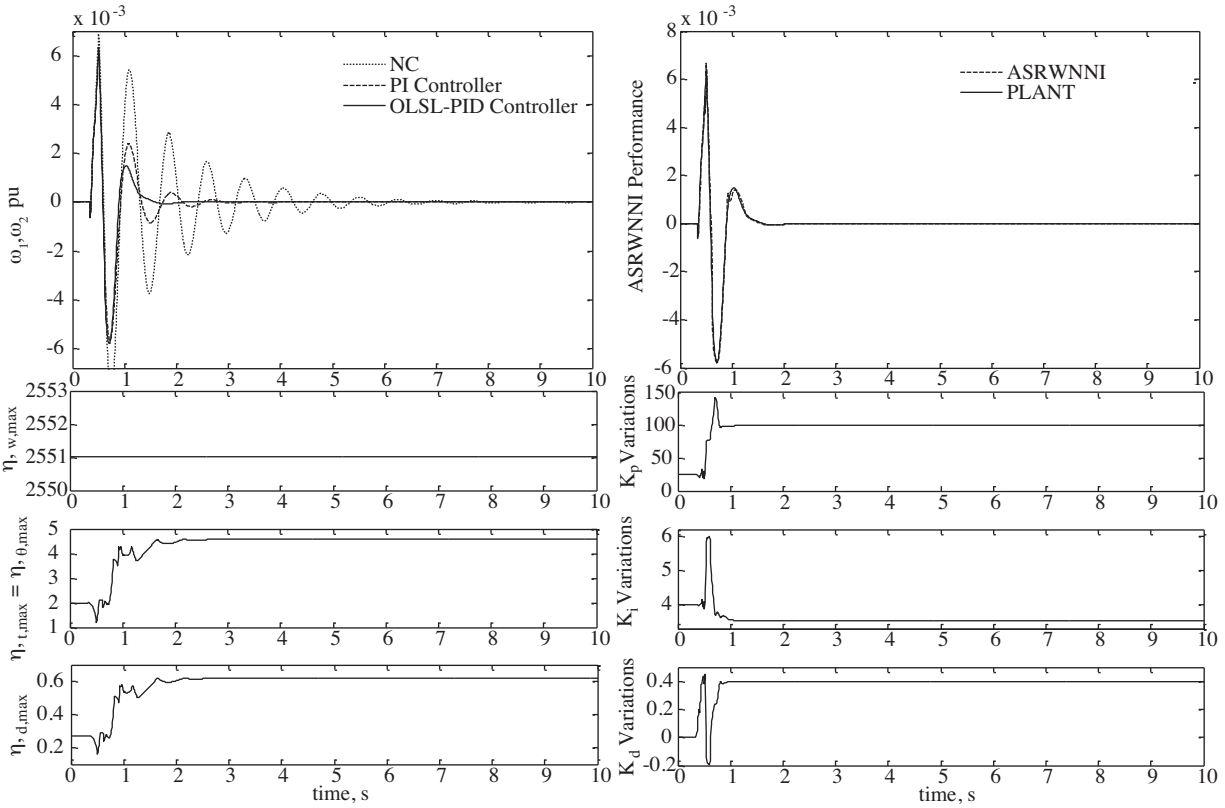

Figure 6. System responses to a 3-phase to ground fault at bus 1 in OP_1.

The second disturbance is a 10% step decrease in the terminal voltage reference of G_1 at time 0.5 s. The system returns to its original condition at time 5 s. Figure 7 shows the system responses and identifier performance.

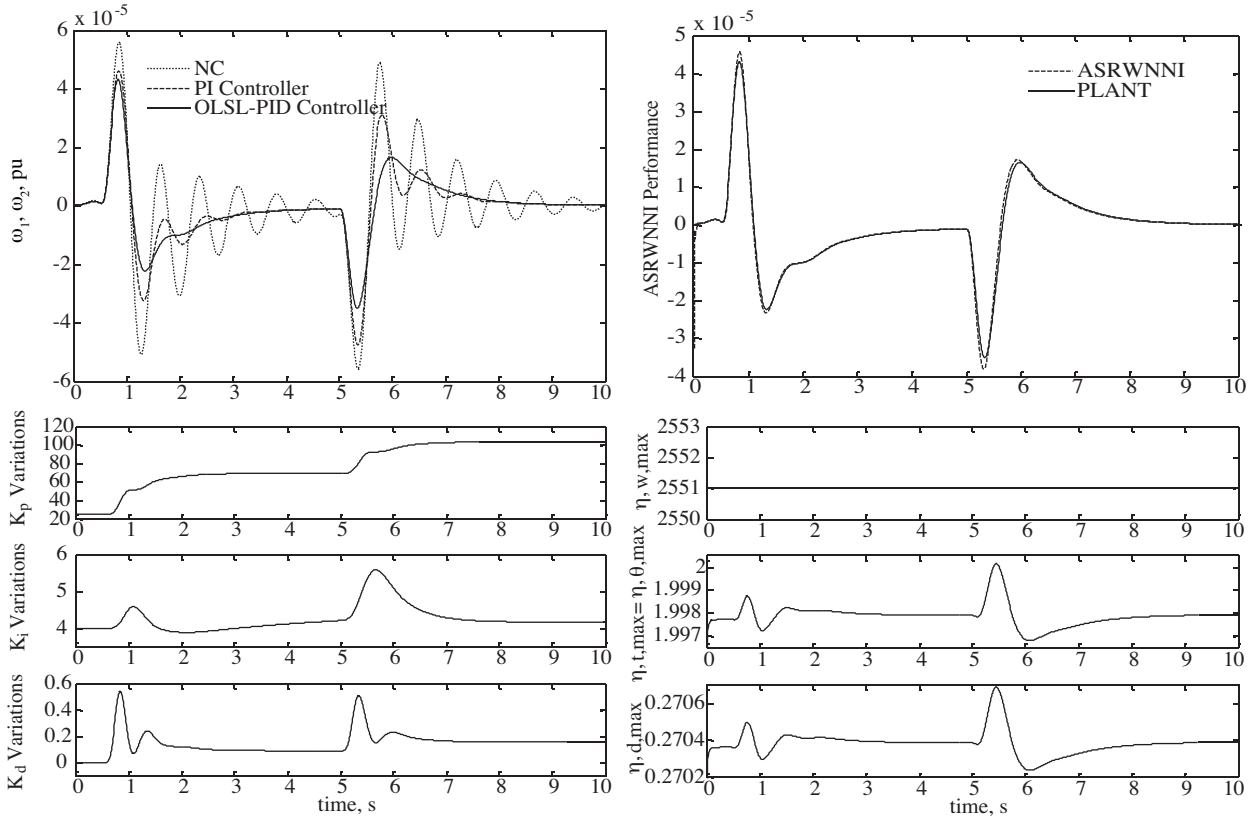

Figure 7. System responses to a 10% step decrease in the voltage reference of G_1 and the return to the original condition in OP_1.

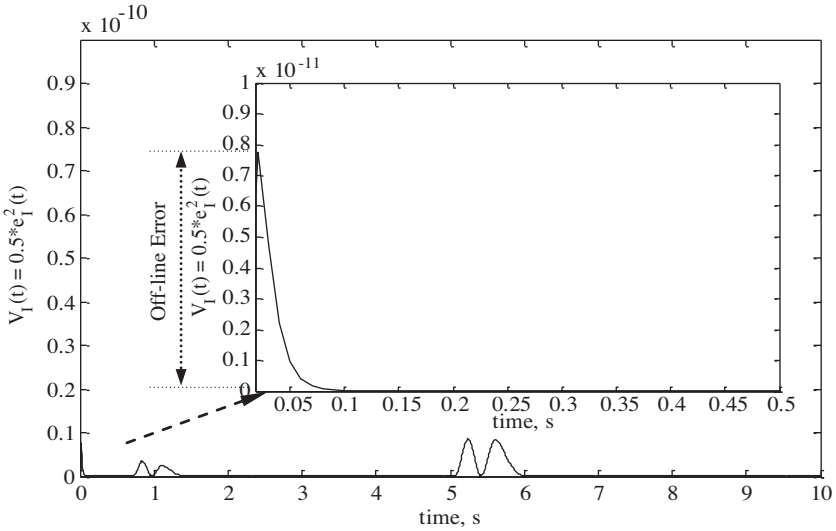

Figure 8. The identification error to a 10% step decrease in the voltage reference of G_1 and the return to the original condition in OP_1.

It can be observed that the proposed controller provides the best performance, damping out the oscillations with a considerable speed. It is also evident that the proposed identifier can track the plant very satisfactorily thanks to its self-recurrent local structure and, likewise, its stable training algorithm. The intelligent changes in the learning rates are another interesting part of the results. The identification error is also provided in Figure 8. From the Lyapunov stability theorem, $V_I(t)$ is expected to have a negative gradient at all times; however, due to the continual control effort, this is practically impossible. In Figure 8 it can be observed that, in the beginning stages of the identification process, the gradient of $V_I(t)$ is negative. This is because the controller output is absent in these stages, and the identifier learning rates are successfully founded by the ALR algorithm and the identifier makes efforts to minimize the off-line training error. Following the fault striking, the PID gains are suddenly changed and the raised control signal is applied to both the plant and the identifier. Sudden changes of the control signal cause the identifier performance to be degraded, and, consequently, the $V_I(t)$ cannot maintain its negative gradient. However, it should be noted that during the control process, the ALR helps the identifier to track the plant with the minimum possible error. At the end of the control process, the control signal is reduced again, and the $V_I(t)$ is effectively decreased with a negative gradient.

6.2.2. The results at OP_2

To test the robustness of the proposed controller, the system loading condition is changed to OP_2. A 3-phase fault of a 10-cycle duration at bus 1 is selected as the first proposed disturbance. The results, including the system responses and identifier performance, are presented in Figure 9. The second disturbance is a 10% step decrease in the terminal voltage reference of G_2 at time 0.5 s. The system returns to its original condition at time 5 s. Figure 10 shows the system responses and the identifier performance.

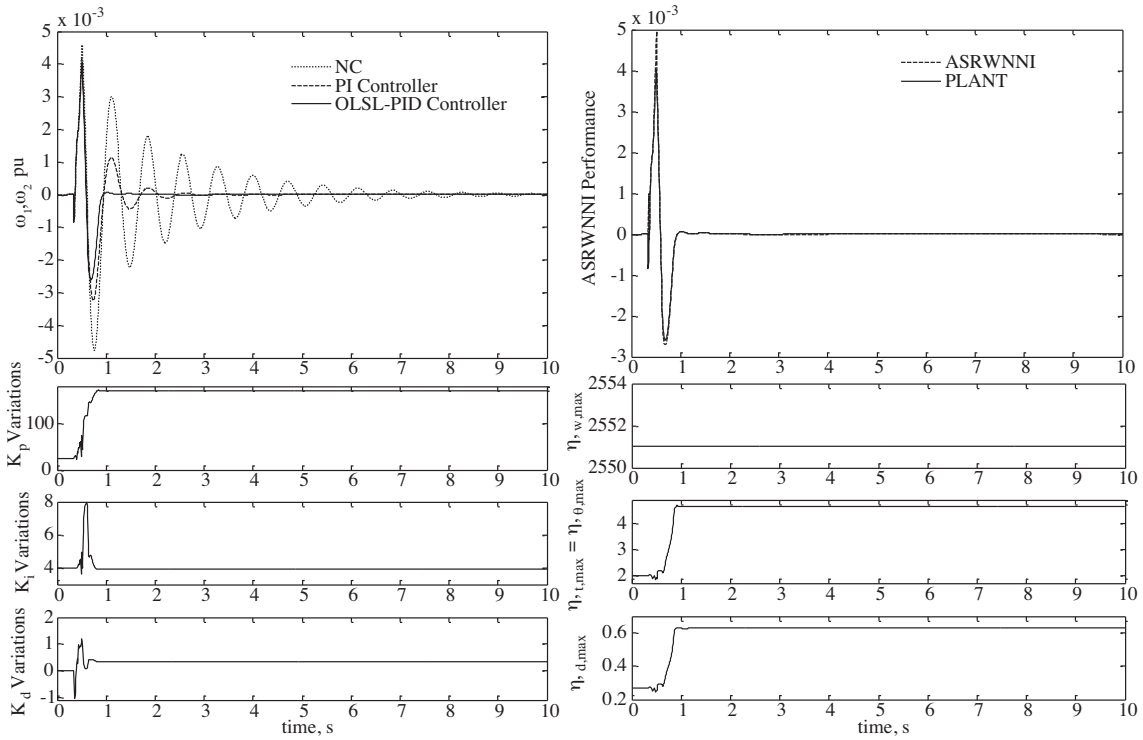

Figure 9. System responses to a 3-phase to ground fault at bus 1 in OP_2.

Again, it is clear from all of the results presented in this section that the proposed approach provides the best control performance for different types of disturbances at different operating points of the system, significantly improving the stability performance of the system despite a considerable change in the system's operating point. It can therefore be concluded that the OLSL-PID controller and the ASRWNNI have acceptable robustness to the operating condition.

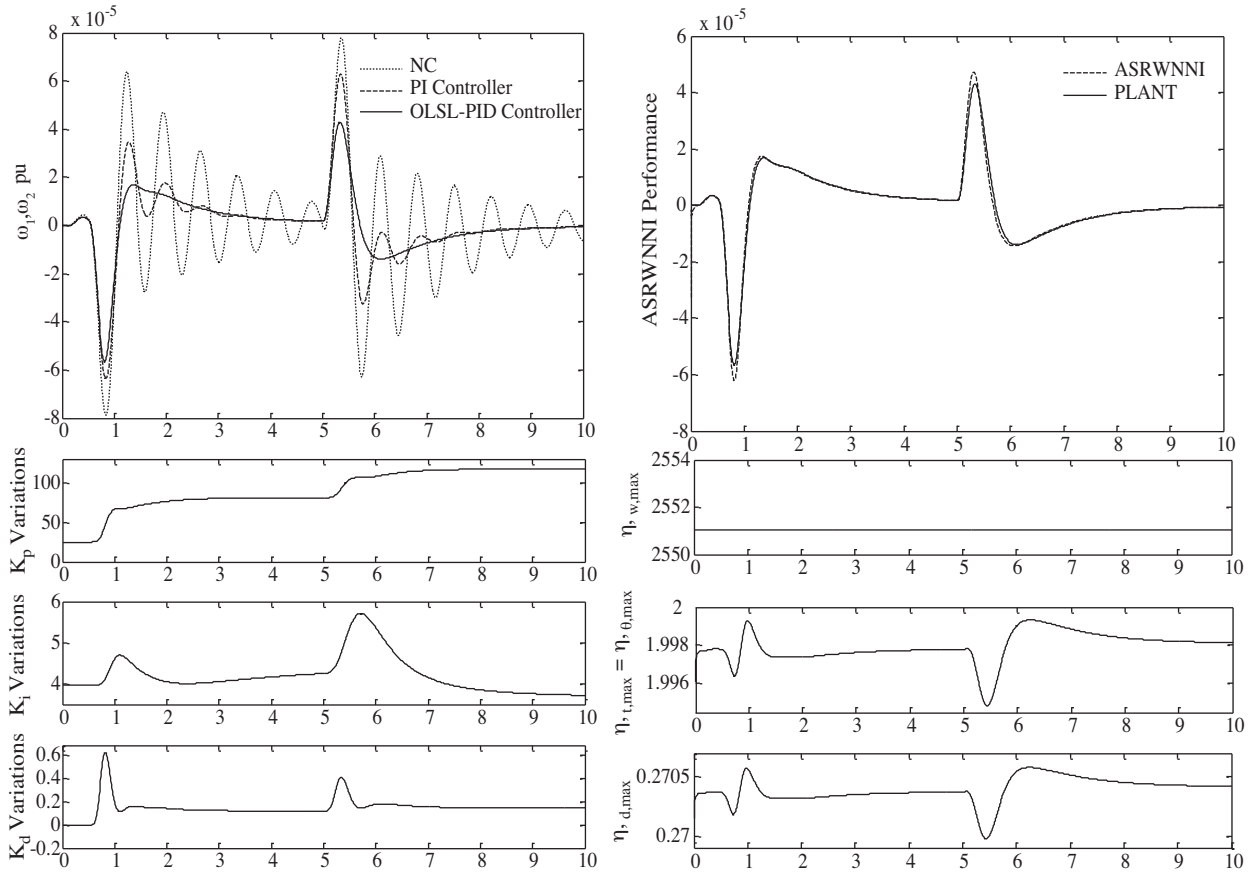

Figure 10. System responses to a 10 % step decrease in the voltage reference of G_2 and the return to the original condition in OP_2.

The identification error to a 10% step decrease in the voltage reference of G_2 and the return to the original condition are provided in Figure 11. Here again, it can be observed that $V_I(t)$ has a negative gradient in the beginning stages of the identification process and the off-line training error is minimized. However, following the fault striking, due to the sudden changes of the PID gains, the identifier performance is degraded, and consequently the $V_I(t)$ cannot maintain its negative gradient. At the end of the control process, the $V_I(t)$ is effectively decreased with a negative gradient.

6.3. Extension to 4-machine, 2-area power system

6.3.1. The 4-machine, 2-area power system with SSSC

A 4-machine, 2-area study system installed with a SSSC, shown in Figure 12, is considered. Each area consists of 2 generator units. The rating of each generator is 900 MVA and 20 kV. Each of the units is connected through

transformers to the 230 kV transmission line. There is a power transfer of 413 MW from area 1 to area 2. Each generator is equipped with a PSS. The detailed data are given in [43].

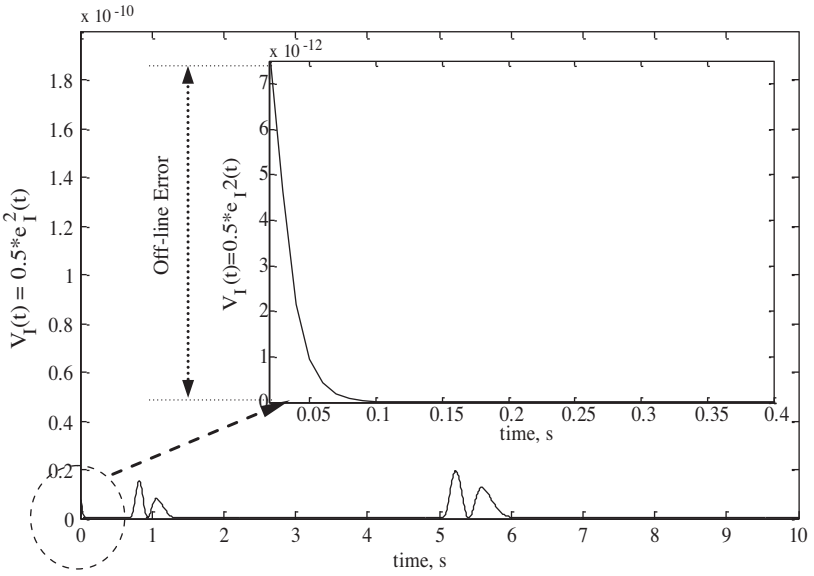

Figure 11. The identification error to a 10% step decrease in the voltage reference of G_2 and return to the original condition in OP_2.

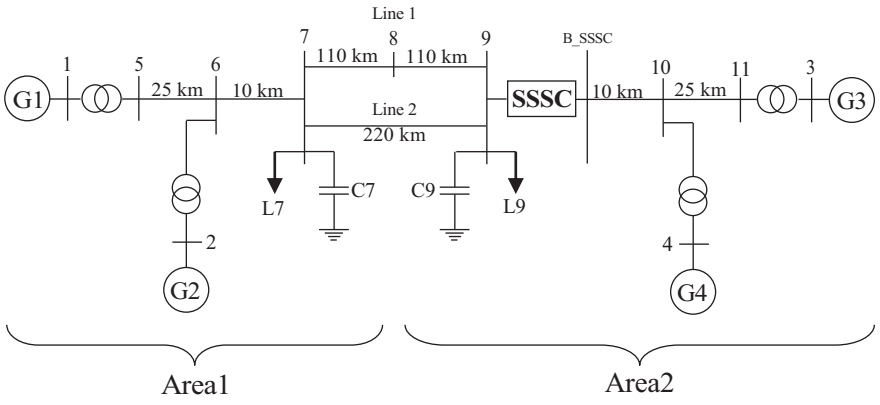

Figure 12. Multimachine power system with a SSSC.

6.3.2. Parameter settings

All of the parameter settings, network structures, and training processes are the same as those of the previous system, the 2-machine, 2-area system. The difference in the speed deviations of generators G_1 and G_3 is selected as the input signal of the proposed controller with the aim of damping the interarea oscillations.

Here again, all of the PID gains are initially set to those of the conventional PI controller. The ASRWNNI is also trained off-line before placing it into the system. All of the input and output signals of the ASRWNNI are scaled to the range of [–1, 1] using parameters α and β (here $\alpha = 0.15$ and $\beta = 0.006$).

6.3.3. Nonlinear time-domain simulation

The system responses to a 3-phase to ground fault of an 8-cycle duration at bus 8 are shown in Figure 13. Figure 14 shows the system responses to a 3-phase to ground fault of an 8-cycle duration at bus 9. The results for a 2-phase to ground fault of an 8-cycle duration at bus 7 are also presented in Figure 15, while Figure 16 shows the system responses to an 8-cycle outage of line 1.

From all of the results presented in this subsection, it can be observed that the proposed controller provides better performance for interarea oscillations damping in comparison to the PI controller, significantly improving the transient stability performance of the system subjected to a wide ranges of disturbances. Acceptable performance of the ASRWNNI for different types of faults can also be deduced from the results.

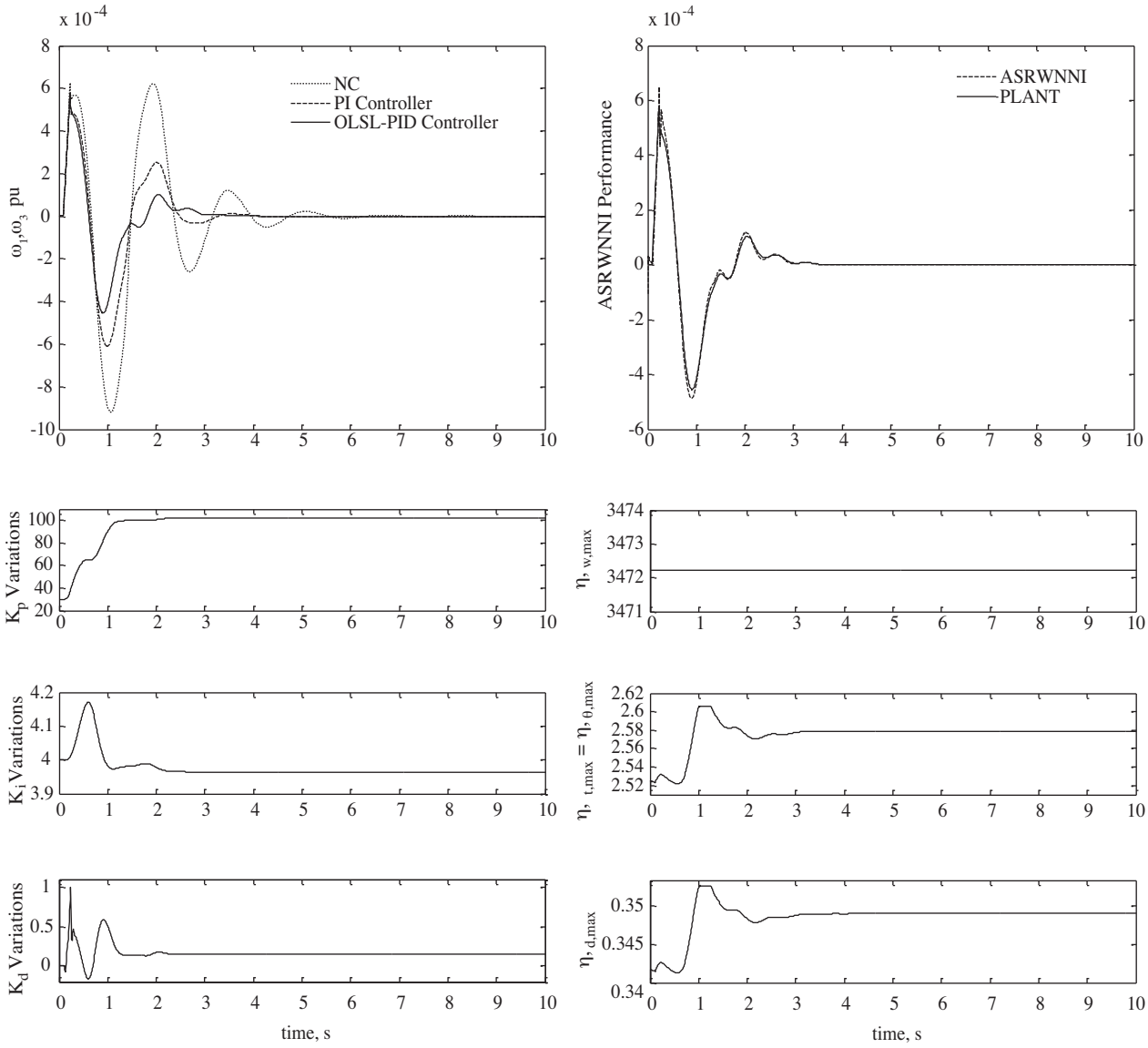

Figure 13. System responses to a 3-phase to ground fault at bus 8.

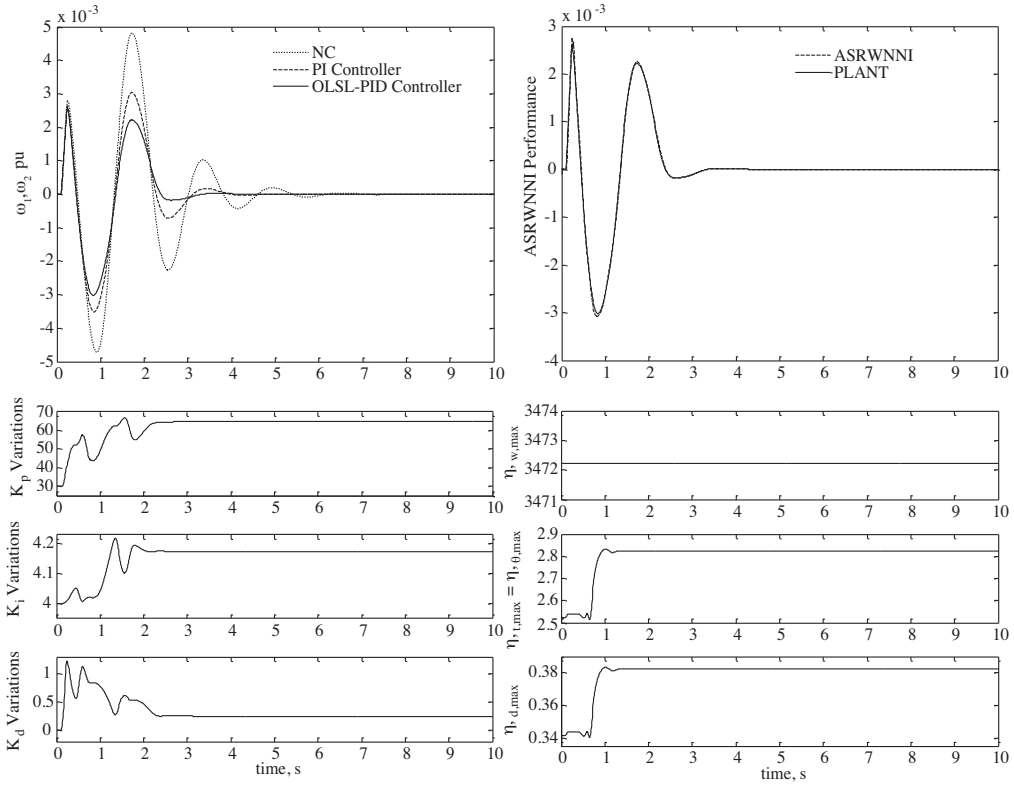

Figure 14. System responses to a 3-phase to ground fault at bus 9.

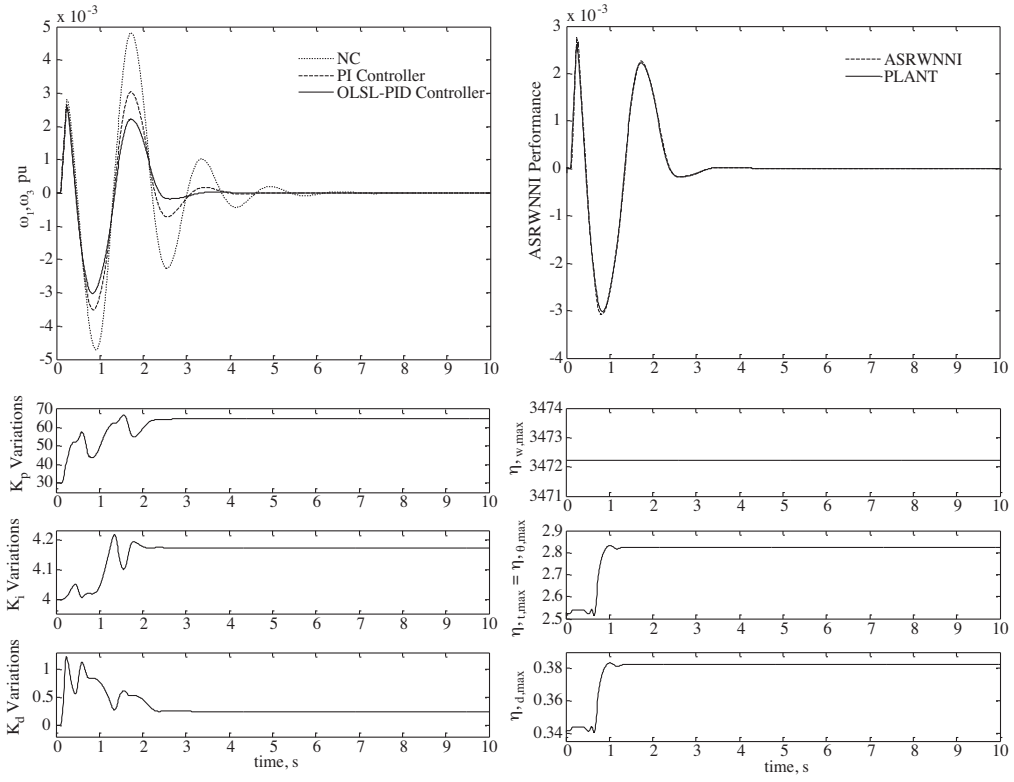

Figure 15. System responses to a 2-phase to ground fault at bus 7.

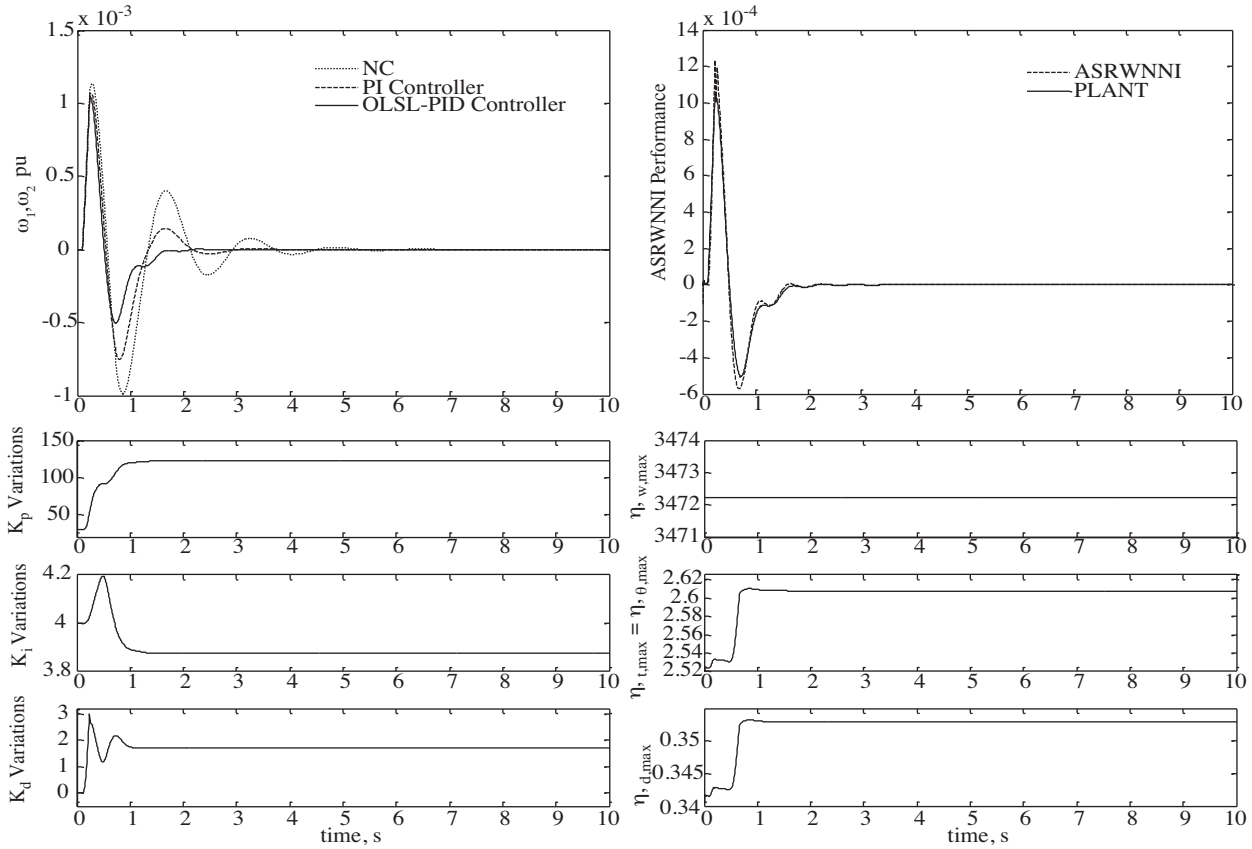

Figure 16. System responses to a 3-phase to 8-cycle outage of line 1.

7. Conclusions

In this article, to overcome the problems of the fixed-gain PI controller of FACTS devices, an OLSL-PID controller was developed for power system stability enhancement. The PID controller parameters were updated based on the information provided by the ASRWNNI, which is a powerful, fast-acting identifier thanks to its local nature, self-recurrent structure, and stable training algorithm with ALRs based on the discrete Lyapunov stability theorem. Following the off-line training of the ASRWNNI, it was placed in the final configuration, and its on-line training was performed in each sampling period. The initial gains of the OLSL-PID were also set to those of a conventional PI controller, and an adapting ability was then added to it by a BP-based on-line updating algorithm. Finally, the proposed control scheme was tested in a 2-machine, 2-area power system under different operating conditions and disturbances. The simulation showed the effectiveness and robustness of the proposed approach, and thus was promising. The design problem was finally extended to a 4-machine, 2-area benchmark power system in order to damp the interarea modes of the oscillations. The results showed that the proposed controller provides better performance for interarea oscillation damping in comparison to the PI controller and they also revealed that because of the high adaptability, the local behavior, and the high flexibility of both the controller and the identifier, the OLSL-PID can damp the oscillations in a good manner and significantly improves the transient stability performance of the system.

Appendix A: System data

Generators: $S_{B1} = 2100$ MVA, $S_{B2} = 1400$ MVA, $H = 3.7$ s, $V_B = 13.8$ kV, $f = 60$ Hz, $R_S = 2.8544$e-3, $X_d = 1.305$, $X'_d = 0.296$, $X"_d = 0.252$, $X_q = 0.474$, $X'_q = 0.243$, $X"_q = 0.18$, $T_d = 1.01$ s, $T'_d = 0.053$ s, $T"_d = 0.1$ s.

Loads: Load1 = 250 MW, Load2 = 100 MW, Load3 = 50 MW.

Transformers: $S_{BT1} = 2100$ MVA, $S_{BT2} = 400$ MVA, 13.8/500 kV, $f = 60$ Hz, $R_1 = R_2 = 0.002$, $L_1 = 0$, $L_2 = 0.12$, D_1/Y_g connection, $R_m = 500$, $L_m = 500$.

Transmission lines: 3-Ph, 60 Hz, line lengths: $L_1 = 280$ km, $L_2 = 300$ km, $L_3 = 50$ km, $R_1 = 0.02546$ Ω/km, $R_0 = 0.3864$ Ω/km, $L_1 = 0.9337$e-3 H/km, $L_0 = 4.1264$e-3 H/km, $C_1 = 12.74$e-9 F/km, $C_0 = 7.751$e-9 F/km.

SSSC: $S_{nom} = 100$ MVA, $V_{nom} = 500$ kV, $f = 60$ Hz, maximum rate of change of reference voltage (V_{qref}) = 3 pu/s; converter impedances: $R = 0.00533$, $L = 0.16$; DC link nominal voltage: $V_{DC} = 40$ kV; DC link equivalent capacitance $C_{DC} = 375$e-6 F; injected voltage regulator gains: $K_P = 0.00375$, $K_i = 0.1875$; DC voltage regulator gains: $K_P = 0.1$e-3, $K_i = 20$e-3; injected voltage magnitude limit: $V_q = \pm 0.2$.

PSSs: PSS_1 and PSS_2: $T_s = 15$e-3, $T_w = 1$, $K_p = 0.25$, $T_1 = 0.06$, $T_2 = 1$, $T_3 = T_4 = 0$.

Appendix B: Adjusting the cycle.

1. If $n = 1$, then go to step B, else:
   (a) Calculate $\partial u(n)/\partial W_c^i(n)$ using Eqs. (4)–(6),
   (b) Update the OLSL-PID gains having the "Data I-a" and $e_c(n+1)$, from the previous time step, using Eqs. (2) and (3).
2. Calculate $u(n)$ and apply it to both the plant and the ASRWNNI.
3. Calculate following items using a SRWNNI:
   (a) $\Delta\hat{y}(n+1)$ using Eq. (11) and then $e_c(n+1)$ (also save $\Delta\hat{y}(n+1)$ to use in the next time step as $\Delta\hat{y}(n)$),
   (b) The system Jacobian $\partial\Delta y(n+1)/\partial u(n)$ using Eq. (18) and save it as "Data I-a",
   (c) Calculate ALRs for ASRWNNI using Eqs. (25)–(27) and save them as "Data I-b",
   (d) Calculate $\partial\Delta\hat{y}(n)/\partial W_I^i(n)$ using Eqs. (14)–(17) and save them as "Data I-c".
4. If $n = 1$, then go to step E, else:
   (a) Calculate $e_I\ (n)$ having $\Delta\hat{y}(n)$ from the previous time step and using the current value of the plant output,
      i. Train the ASRWNNI having "Data I-b" and "Data I-c" from the previous time step, using Eq. (13).
5. Go to (A) for the next time step.

A. Appendix C: The proof of Theorem 1.

A discrete-type Lyapunov function can be given by:

$$V_I(n) = \frac{1}{2}e^2(n), \tag{C.1}$$

where $e(n) = (y(n) - \hat{y}(n))$ represents the error in the learning process. Then:

$$\begin{aligned} \Delta V_I(n) &= V_I(n+1) - V_I(n) \\ &= \frac{1}{2}\left[e^2(n+1) - e^2(n)\right] \end{aligned}. \tag{C.2}$$

The error difference can be represented by:

$$\begin{aligned} e(n+1) &= e(n) + \Delta e(n) \\ &\approx e(n) + \left[\frac{\partial e(n)}{\partial W_I^i}\right]^T \Delta W_I^i \end{aligned}, \tag{C.3}$$

and also:

$$\Delta W_I^i = \eta_I^i \left(-\frac{\partial J_I(n)}{\partial W_I^i}\right) = \eta_I^i e(n) \frac{\partial \hat{y}(n)}{\partial W_I^i}. \tag{C.4}$$

Next, from Eqs. (C.2)–(C.4), $\Delta V_I(n)$ can be represented as:

$$\Delta V_I(n) = \Delta e(n)\left(e(n) + \frac{1}{2}\Delta e(n)\right) = -\lambda e^2(n),$$

where

$$\lambda = \frac{1}{2}\eta_I^i \left\|g^i(n)\right\|^2 \left(2 - \eta_I^i \left\|g^i(n)\right\|^2\right). \tag{C.5}$$

If $\lambda > 0$ is satisfied, $\Delta V_I(n) < 0$. Thus, the asymptotic convergence of the proposed identifier is guaranteed. Let $\eta_\alpha = \eta_I^i (g_{max}^i)^2$ [33], and then:

$$\lambda \geq \frac{1}{2}\eta_I^i \left\|g^i(n)\right\|^2 (2 - \eta_\alpha) > 0. \tag{C.6}$$

From Eq. (C.6), we obtain $0 < \lambda_\alpha < 2$ and Eq. (21) follows. This completes the proof. □

B. Appendix D: The proof of Theorem 2.

$g^w(n) = \partial\hat{y}(n)/\partial w$, and then we have:

$$g^w(n) = \sum_{i=1}^{N_w} \psi_i.$$

Since we have $\psi_i \leq 1$ for all i,

$$\|g^w(n)\| < \sqrt{N_w} \xrightarrow{\text{So we have}} (g_{\max}^w)^2 = N_w.$$

Accordingly, from Theorem 1, we obtain $0 < \eta_I^w < 2 / N_w$. This completes the proof. □

C. Appendix E: The proof of Theorem 3.

In order to prove Theorem 3, the following lemmas are used [33,40].

Lemma 1. *Let* $f(r) = r.\ \exp(-r^2)$. *Then,* $|f(r)| < 1\ \forall r \in \Re$.

Lemma 1. *Let g(r)* $= r^2.\ \exp(-r^2)$. *Then,* $|\ \mathrm{g}(r)| < 1\ \forall r \in \Re$.

(A). $g^t(n) = \partial\hat{y}(n)/\partial t$, and then we have:

$$\begin{aligned} g^t(n) &= \sum_{i=1}^{N_w} w_i \left(\frac{\partial \psi_i}{\partial t}\right) \\ &= \sum_{i=1}^{N_w} w_i \left\{\sum_{j=1}^{N_i} \left(\frac{\partial \phi(z_{ij})}{\partial z_{ij}} \frac{\partial z_{ij}}{\partial t}\right)\right\} \\ &< \sum_{i=1}^{N_w} w_i \left\{\sum_{j=1}^{N_i} \max\left(-2\alpha.\exp(-0.5-\alpha) \times \tfrac{-1}{d}\right)\right\}, \end{aligned}$$

where $\alpha = \left(z_{ij}^2 - 1\right)/2$, and according to Lemma 2 $|\alpha.\exp(-\alpha)| < 1$; then we have:

$$\left\|g^t(n)\right\| < \sqrt{N_w}\sqrt{N_i}\,|w|_{\max} \frac{2\exp(-0.5)}{|d|_{\min}}.$$

Then:

$$\left(g_{\max}^t\right)^2 = N_w N_i \left[\frac{|w|_{\max} \times 2\exp(-0.5)}{|d|_{\min}}\right]^2.$$

Accordingly, from Theorem 1, we obtain Eq. (22).

(B). $g^d(n) = \partial\hat{y}(n)/\partial d$, and then we have:

$$\begin{aligned} g^d(n) &= \sum_{i=1}^{N_w} w_i \left(\frac{\partial \psi_i}{\partial d}\right) \\ &= \sum_{i=1}^{N_w} w_i \left\{\sum_{j=1}^{N_i} \left(\frac{\partial \phi(z_{ij})}{\partial z_{ij}} \frac{\partial z_{ij}}{\partial d}\right)\right\} \\ &< \sum_{i=1}^{N_w} w_i \left\{\sum_{j=1}^{N_i} \max\left(\frac{-2\alpha.z_{ij}\exp\left(0.5-\alpha-z_{ij}^2\right)}{d}\right)\right\}, \end{aligned}$$

where $\alpha = \left(1 - z_{ij}^2\right)/2$, and so according to Lemmas 1 and 2 $\left|z_{ij}\exp\left(-z_{ij}^2\right)\right| < 1$ and $|\alpha.\exp(-\alpha)| < 1$, and then we have:

$$\left\|g^d(n)\right\| < \sqrt{N_w}\sqrt{N_i}\,|w|_{\max} \frac{2\exp(0.5)}{|d|_{\min}}.$$

Then:

$$\left(g_{\max}^d\right)^2 = N_w N_i \left[\frac{|w|_{\max} \times 2\exp(0.5)}{|d|_{\min}}\right]^2.$$

Accordingly, from Theorem 1, we obtain Eq. (23).

(C). $g^{\theta}(n) = \partial\hat{y}(n)/\partial\theta$, and then we have:

$$\begin{aligned} g^{\theta}(n) &= \sum_{i=1}^{N_w} w_i \left(\frac{\partial\psi_i}{\partial\theta}\right) \\ &= \sum_{i=1}^{N_w} w_i \left\{\sum_{j=1}^{N_i}\left(\frac{\partial\phi(z_{ij})}{\partial z_{ij}}\frac{\partial z_{ij}}{\partial\theta}\right)\right\} \\ &< \sum_{i=1}^{N_w} w_i \left\{\sum_{j=1}^{N_i}\max\left(-2\alpha.\exp(-0.5-\alpha)\times\frac{\phi_{ij}(n-1)}{d}\right)\right\}, \end{aligned}$$

where $\alpha = \left(z_{ij}^2 - 1\right)/2$, and according to Lemma 2 $|\alpha.\exp(-\alpha)| < 1$, and then we have:

$$\left\|g^{\theta}(n)\right\| < \sqrt{N_w}\sqrt{N_i}\,|w|_{\max}\frac{2\exp(-0.5)}{|d|_{\min}}.$$

Then:

$$\left(g_{\max}^{\theta}\right)^2 = N_w N_i\left[\frac{|w|_{\max}\times 2\exp(-0.5)}{|d|_{\min}}\right]^2.$$

Accordingly, from Theorem 1, we obtain Eq. (24). This completes the proof. □

D. Appendix F: PI controller parameters

Table F. PID (PI) optimal gains.

K_p	K_i	K_d
23.86	3.98	0

References

[1] P.W. Sauer, M.A. Pai, Power System Dynamic and Stability, Hoboken, NJ, Prentice Hall, 1998.

[2] M.R. Banaei, A. Kami, "Interline power flow controller (IPFC) based damping recurrent neural network controllers for enhancing stability", Energy Conversion and Management, Vol. 52, pp. 2629–2636, 2011.

[3] A.T. Al-Awami, Y.L. Abdel-Magid, M.A. Abido, "A particle-swarm-based approach of power system stability enhancement with unified power flow controller", International Journal of Electrical Power & Energy Systems, Vol. 29, pp. 251–259, 2007.

[4] H. Shayeghi, H.A. Shayanfar, S. Jalilzadeh, A. Safari, "A PSO based unified power flow controller for damping of power system oscillations", Energy Conversion and Management, Vol. 50, pp. 2583–2592, 2009.

[5] H. Shayeghi, H.A. Shayanfar, S. Jalilzadeh, A. Safari, "Design of output feedback UPFC controller for damping of electromechanical oscillations using PSO", Energy Conversion and Management, Vol. 50, pp. 2554–2561, 2009.

[6] H. Shayeghi, H.A. Shayanfar, S. Jalilzadeh, A. Safari, "Tuning of damping controller for UPFC using quantum particle swarm optimizer", Energy Conversion and Management, Vol. 51, pp. 2299–2306, 2010.

[7] M. Vilathgamuwa, X. Zhu, S.S. Choi, "A robust control method to improve the performance of a unified power flow controller", Electric Power Systems Research, Vol. 55, pp. 103–111, 2000.

[8] M.R. Banaei, A.R. Kami, "Improvement of dynamical stability using interline power flow controller", Advances in Electrical and Computer Engineering, Vol. 10, pp. 42–49, 2010.

[9] S. Panda, "Robust coordinated design of multiple and multi-type damping controller using differential evolution algorithm", International Journal of Electrical Power & Energy Systems, Vol. 33, pp. 1018–1030, 2011.

[10] S. Panda, "Multi-objective evolutionary algorithm for SSSC-based controller design", Electric Power Systems Research, Vol. 79, pp. 937–944, 2009.

[11] A. Kazemi, M.V. Sohrforouzani, "Power system damping using fuzzy controlled facts devices", Electrical Power and Energy Systems, Vol. 28, pp. 349–357, 2006.

[12] N.G. Hingorani, L. Gyugyi, Understanding FACTS Concepts and Technology of Flexible AC Transmission System, New York, IEEE Press, 2000.

[13] K.J. Astrom, T. Hagglund, C.C. Hang, W.K. Ho, "Automatic tuning and adaptation for PID controllers – a survey", Control Engineering Practice, Vol. 1, pp. 699–714, 1993.

[14] P. Cominos, N. Munro, "PID controllers: recent tuning methods and design to specification", IEE Proceedings - Control Theory and Applications, Vol. 149, pp. 46–53, 2002.

[15] J.G. Ziegler, N.B. Nichols, "Optimum setting for automatic controllers", Transactions of the ASME, Vol. 64, pp. 759–765, 1942.

[16] W.K. Ho, C.C. Hang, L.S. Cao, "Tuning of PID controllers based on gain and phase margin specifications", Automatica, Vol. 31, pp. 497–502, 1995.

[17] A.J. Isakson, S.F. Graebe, "Analytical PID parameter expressions for higher order systems", Automatica, Vol. 35, pp. 1121–1130, 1999.

[18] S. Skogestad, "Simple analytic rules for model reduction and PID controller tuning", Journal of Process Control, Vol. 13, pp. 291–309, 2003.

[19] B. Kristiansson, B. Lennartson, "Robust and optimal tuning of PI and PID controllers", IEE Proceedings - Control Theory and Applications, Vol. 149, pp. 17–25, 2002.

[20] E. Grassi, K. Tsakalis, S. Dash, S.V. Gaikwad, W. Macarthur, G. Stein, "Integrated system identification and PID controller tuning by frequency loop-shaping", IEEE Transactions on Control Systems Technology, Vol. 9, pp. 285–294, 2001.

[21] C. Lin, Q.G. Wang, T.H. Lee, "An improvement on multivariable PID controller design via iterative LMI approach", Automatica , Vol. 40, pp. 519–525, 2004.

[22] F. Zheng, Q.G. Wang, T.H. Lee, "On the design of multivariable PID controllers via LMI approach", Automatica, Vol. 38, pp. 517–526, 2002.

[23] M.T. Ho, "Synthesis of H1 PID controllers: a parametric approach", Automatica, Vol. 39, pp. 1069–1075, 2003.

[24] S.J. Ho, L.S. Shu, S.Y. Ho, "Optimizing fuzzy neural networks for tuning PID controllers using an orthogonal simulated annealing algorithm OSA", IEEE Transactions on Fuzzy Systems, Vol. 14, pp. 421–434, 2006.

[25] C. Vlachos, D. Williams, J.B. Gomm, "Solution to the Shell standard control problem using genetically tuned PID controllers", Control Engineering Practice, Vol. 10, pp. 151–163, 2002.

[26] C.C. Kao, C.W. Chuang, R.F. Fung, "The self-tuning PID control in a slider-crank mechanism system by applying particle swarm optimization approach", Mechatronics, Vol. 16, pp. 513–522, 2006.

[27] L.D.S. Coelho, "Tuning of PID controller for an automatic regulator voltage system using chaotic optimization approach", Chaos, Solitons & Fractals, Vol. 39, pp. 1504–1514, 2009.

[28] P. Shamsollahi, O.P Malik, "An adaptive power system stabilizer using on-line trained neural networks", IEEE Transactions on Energy Conversion, Vol. 12, pp. 382–387, 1997.

[29] P. Shamsollahi, O.P Malik, "Direct neural adaptive control applied to synchronous generator", IEEE Transactions on Energy Conversion, Vol. 14, pp. 1341–1346, 1999.

[30] J. He, O.P. Malik, "An adaptive power system stabilizer based on recurrent neural networks", IEEE Transactions on Neural Networks, Vol. 12, pp. 413–418, 1997.

[31] T. Kobayashi, A. Yokoyama, "An adaptive neuro-control system of synchronous generator for power system stabilization", IEEE Transactions on Energy Conversion, Vol. 11, pp. 621–630, 1996.

[32] W. Liu, G.K. Venayagamoorthy, D.C. Wunsch 2nd, "Adaptive neural network based power system stabilizer design", INNS-IEEE International Joint Conference on Neural Networks, pp. 2970–2975, 2003.

[33] S.J. Yoo, J.B. Park, Y.H. Choi, "Stable predictive control of chaotic systems using self-recurrent wavelet neural network", International Journal of Control, Automation, and Systems, Vol. 3, pp. 43–55, 2005.

[34] R.J. Wai, J.M. Chang, "Intelligent control of induction servo motor drive via wavelet neural network", Electric Power Systems Research, Vol. 61, pp. 67–76, 2002.

[35] Y. Oussar, I. Rivals, L. Personnaz, G. Dreyfus, "Training wavelet networks for nonlinear dynamic input-output modeling", Neurocomputing, Vol. 20, pp. 173–188, 1998.

[36] J. Zhang, G. Walter, Y. Miao, W.N.W. Lee, "Wavelet neural networks for function learning", IEEE Transactions on Signal Processing, Vol. 43, pp. 1485–1497, 1995.

[37] Q. Zhang, A. Benveniste, "Wavelet networks", IEEE Transactions on Neural Networks, Vol. 3, pp. 889–898, 1992.

[38] Y. Oussar, G. Dreyfus, "Initialization by selection for wavelet network training", Neurocomputing, Vol. 34, pp. 131–143, 2000.

[39] Lekutai G, "Adaptive self-tuning neuro wavelet network controllers", PhD, Virginia Polytechnic Institute and State University, Blacksburg, VA, USA, 1997.

[40] S.J. Yoo, J.B. Park, Y.H. Choi, "Indirect adaptive control of nonlinear dynamic systems using self-recurrent wavelet neural networks via adaptive learning rates", Information Sciences, Vol. 177, pp. 3074–3098, 2007.

[41] K.S. Narendra, K. Parthasarathy, "Identification and control of dynamic system using neural network", IEEE Transactions on Neural Networks, Vol. 1, pp. 4–27, 1990.

[42] K.S. Narendra, K. Parthasarathy, "Gradient methods for the optimization of dynamical systems containing neural networks", IEEE Transactions on Neural Networks, Vol. 2, pp. 252–262, 1991.

[43] P. Kundur, Power System Stability and Control, New York, McGraw-Hill, 1993.